Grafting Poly(4-vinylpyridine) with a Second-Order Nonlinear Optically Active Nickel(II) Chromophore

Ugo Caruso,[a] Roberto Centore,*[a] Barbara Panunzi,[b] Antonio Roviello,*[a] and Angela Tuzi[a]

Keywords: N ligands / Nickel / Nonlinear optics / Poly(4-vinylpyridine)

Metal-containing polymers are obtained by grafting commercial poly(4-vinylpyridine) (average molecular weight 60000 or 160000) with a Ni^{II} chromophore complex. The metal-containing chromophore was obtained from a tridentate benzoylhydrazine ligand. Chromophore fragments were grafted onto the polymer by formation of a coordinative bond between the metal and the pyridinic nitrogen. Two acentric mononuclear Ni^{II} complexes containing pyridine as an additional ligand, in a square-planar or in an octahedral environment, have been prepared and characterised also by single-crystal X-ray analysis. The chemical and thermal properties of the model complexes and of the grafted polymers were examined and compared with those of Cu^{II}- and Pd^{II}-based ones, in particular with reference to their NLO properties.

Introduction

Metallopolymers are a very attractive class of materials because of their widespread applications.[1a–1c] In particular, polymers bearing metallic chromophores are of current interest in the area of nonlinear optically (NLO) active materials.[2a,2b] Considerable effort has been directed toward molecular engineering of second order NLO-active coordination complexes that can be covalently bonded to a polymeric system. There are many examples in the recent literature of polymers with a metal-containing chromophoric moiety in the main chain or as side groups.[3a–3c] In particular, researchers aim to produce materials with high NLO responses that are easy to synthesise and are chemically and thermally stable.

Recently, we have developed a new approach to second-order NLO active metallopolymers based on grafting metallochromophores onto preformed (and commercially available) coordinating polymers, such as poly(4-vinylpyridine).[4a–4c] Metallochromophores are obtained by coordination of suitable metal ions to push-pull *N*-salicylidene-*N′*-aroylhydrazine-type tridentate ligands. An example of a polymer based on this approach is shown in Scheme 1 (M = metal atom).

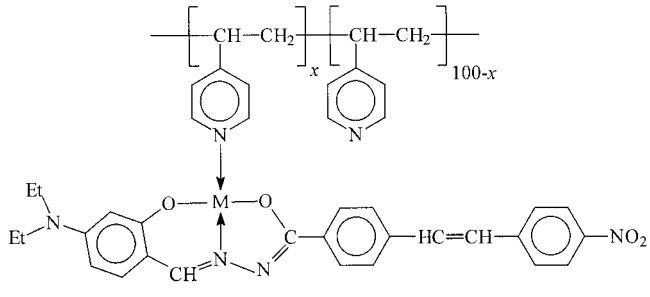

Scheme 1.

It is likely that the coordination properties of the metal have an effect on the properties of the grafted polymer. In fact, in the case of expansion of the coordination sphere of the metal from square planar to penta- or hexacoordinate environments, a partial cross-linking (by coordination) can occur in the polymer system. This, in turn, should affect some polymer properties related to second order NLO applications, such as the glass-transition temperature and the time stability of the orientational order induced during the poling process and its extent. Up to now we have restricted our investigation to Cu^{II}- and Pd^{II}-containing metallopolymers, for which the coordination geometry expected and most frequently found is square planar, so that coordinative cross-linking of the polymers should not be expected. Actually, for model complexes of Cu^{II} with some ligands having a longer conjugation path, crystallographic evidence for weak interaction of the square-planar coordinated metal with an additional pyridine molecule, leading to pseudo-pentacoordinate complexes, has been observed.[4a–4c]

[a] Dipartimento di Chimica, Università degli Studi di Napoli "Federico II",
Via Cinthia, 80126 Napoli, Italy
E-mail: roberto.centore@unina.it
antonio.roviello@unina.it
[b] Dipartimento di Scienza degli Alimenti, Università degli Studi di Napoli "Federico II",
Via Università 100, 80155 Portici, Napoli, Italy

To the best of our knowledge, only a few reports of nickel-based NLO active polymers have appeared,[5a–5c] and some of these deal with host–guest-type systems.[6a,6b] In this paper we report a detailed investigation of the polymer system shown in Scheme 1 and containing Ni^{II} as the metal ion, for which a greater relevance of hexacoordination of the metal can be expected. In addition, the crystal structures of the model complexes (pyridine adducts) shown in Scheme 2 are also reported.

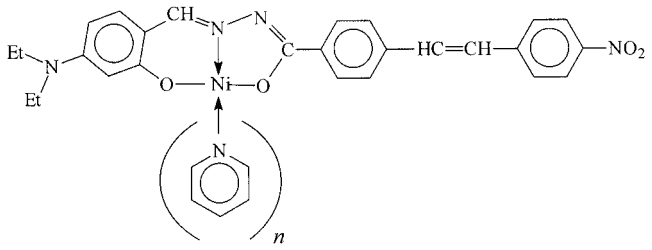

Scheme 2.

Results and Discussion

A general outline of the synthetic route to the new nickel-grafted polymers is shown in Scheme 3.

The model complex [Ni(L)Py] was synthesised as described in the Experimental Section. Its DSC heating curve shows only a broad endothermic signal starting at about 250 °C, corresponding to loss of the coordinated pyridine. No melting was observed under the polarizing microscope up to decomposition (about 345 °C, as detected by TGA analysis). The second-order molecular nonlinearity of [Ni(L)Py] was determined by the EFISH technique. The result obtained, $\mu\beta = 850 \times 10^{-48}$ esu, indicates a moderate activity and is consistent with results we have reported for Cu^{II} and Pd^{II} complexes containing the same ligand or closely related ligands ($\mu\beta$ between 1100×10^{-48} and 1500×10^{-48} esu[4a,4c]).

Recrystallisation of [Ni(L)Py] from THF/hexane gave brick-red prismatic crystals suitable for X-ray analysis that confirmed the square-planar coordination of nickel by the tridentate ligand and one pyridine molecule; a solvent (THF) molecule is also included in the crystal lattice. Remarkably, the same complex, when recrystallised by evaporation from pyridine, gave dark-violet crystals that, in about two hours at room temperature, turned to dark red, undergoing about 33% weight loss. Subsequent structural analysis confirmed that the dark-violet crystals contain the hexacoordinate complex [Ni(L)Py_3], in which two additional pyridine molecules are coordinated to the metal in apical positions, and pointed out the presence of a large amount of solvent of crystallisation in the crystals (2.5 pyridine molecules for each complex molecule). Since the crystals easily lose the solvent at room temperature, and also some coordinated pyridine on heating, as evidenced by the complex TGA pattern, the X-ray structural analysis for this complex was necessarily performed at low temperature (–100 °C).

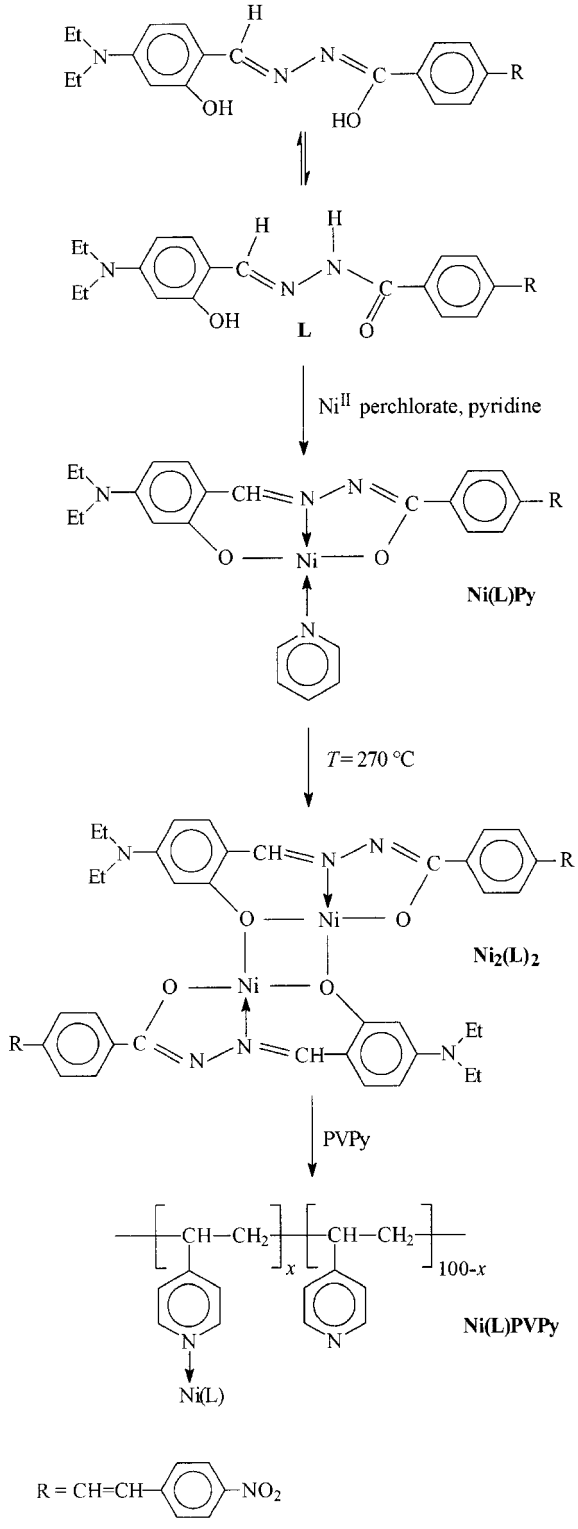

Scheme 3.

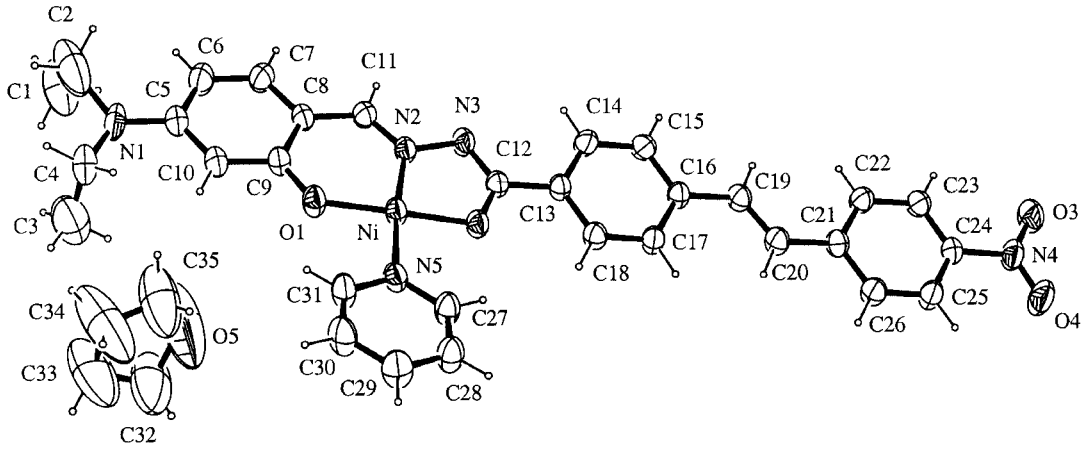

Figure 1. ORTEP view of [Ni(L)Py]. Thermal ellipsoids are at the 30% probability level. The THF solvent molecule is also shown.

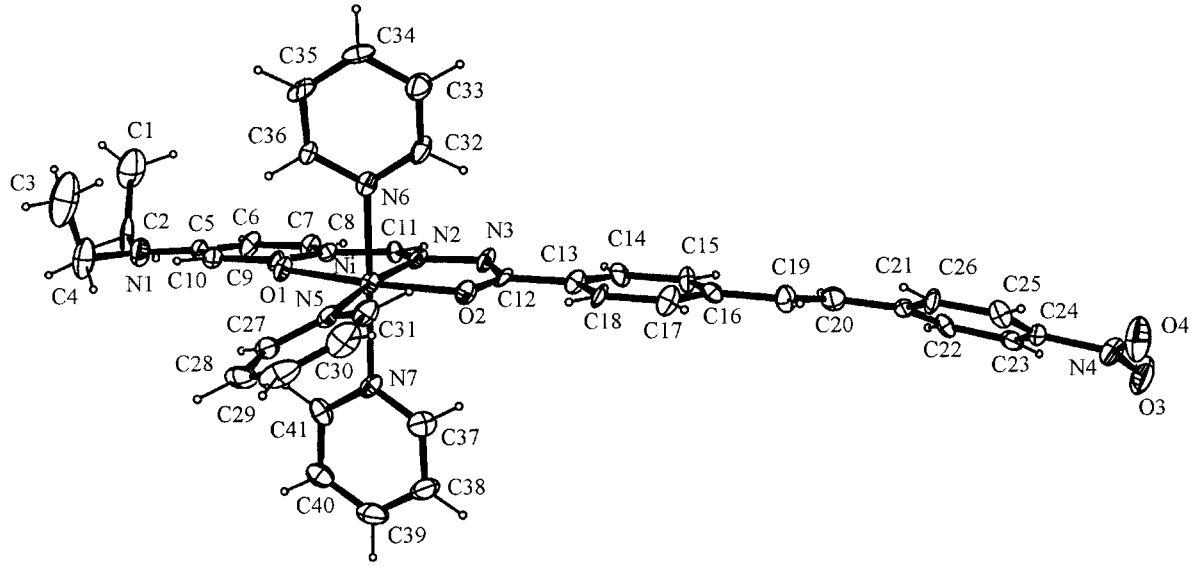

Figure 2. ORTEP view of [Ni(L)Py_3]. Thermal ellipsoids are at the 30% probability level. Pyridine solvent molecules are not shown.

The molecular structures of complexes [Ni(L)Py] and [Ni(L)Py_3] are shown in Figures 1 and 2 respectively. Selected bond lengths and angles are given in Table 1.

As evidenced by the C–O and C–N bond lengths (see Table 1), and in accordance with analogous compounds,[4a–4c] the tridentate ligand is present in its enol form in both complexes. It adopts a substantially planar conformation in the first complex, while a small torsion of the nitrophenyl group around the C20–C21 bond is present in the second (see Table 1). The coordination geometry is different in the two complexes: it is square planar in [Ni(L)Py], with general geometric features very close to those observed for analogous Cu^{II} and Pd^{II} compounds,[4a–4c] whereas in [Ni(L)Py_3] the metal is hexacoordinate with a fairly regular octahedral coordination geometry, with the tridentate ligand and one pyridine in the equatorial positions, while two additional pyridine molecules occupy the axial positions at the same mean distance (shorter than those recorded for analogous pseudo-pentacoordinate Cu^{II} complexes[4a–4c]). As compared to the square-planar complex, the distances between the metal and ligands are slightly longer in the octahedral complex, as expected. The mean plane of the (N5, C27–C31) coordinated pyridine is twisted by about 22° with respect to the equatorial coordination plane, while the mean planes of the two axial pyridines are twisted by about 18° with respect to each other. Solvent molecules are present in the crystal packing of both compounds, and this seems to be necessary in order to get crystallisation. In particular, in [Ni(L)Py_3] the pyridine solvent molecules are placed into channels running parallel to the *c* axis across the crystal, and this could explain why these molecules are easily lost even at room temperature. One pyridine solvent molecule lies on the binary axis along *c*, while the other two are placed near the screw axis parallel to *c*. Although crystals of [Ni(L)Py_3] are acentric (space group *Fdd*2), no relevant NLO activity

Table 1. Selected bond lengths [Å], bond angles [°] and torsion angles [°] for [Ni(L)Py] and [Ni(L)Py_3] with esd's in parentheses.

	[Ni(L)Py]	[Ni(L)Py_3]
Ni–O1	1.817(4)	2.016(5)
Ni–O2	1.840(3)	2.051(5)
Ni–N2	1.822(4)	1.995(6)
Ni–N5	1.948(5)	2.104(7)
Ni–N6		2.158(6)
Ni–N7		2.195(6)
O1–C9	1.310(6)	1.312(8)
O2–C12	1.298(6)	1.270(9)
N2–C11	1.279(6)	1.277(8)
N3–C12	1.305(6)	1.326(10)
O1–Ni–N2	95.4(2)	91.9(3)
O2–Ni–N2	83.2(2)	79.2(2)
O1–Ni–N5	89.8(2)	95.2(3)
O2–Ni–N5	91.8(2)	93.7(3)
O2–Ni–N6		89.5(2)
N2–Ni–N6		94.6(2)
N5–Ni–N6		87.9(2)
O2–Ni–N7		89.7(2)
N2–Ni–N7		90.5(2)
N5–Ni–N7		86.9(2)
N6–Ni–N7		174.6(2)
C11–N2–N3–C12	–177.2(5)	–170.8(6)
C7–C8–C11–N2	178.1(6)	–178.0(7)
N3–C12–C13–C18	–172.4(5)	175.5(7)
C15–C16–C19–C20	–177.7(5)	–5.6(13)
C19–C20–C21–C26	174.5(5)	–16.5(8)
O1–Ni–N5–C27	178.4(4)	28.5(6)
O1–Ni–N6–C32		–157.2(6)
O1–Ni–N7–C37		175.2(6)

is expected for them because the molecules are elongated perpendicularly to the polar binary axis, which gives rise to an antiparallel arrangement of the push–pull fragments.

As far as the thermal behaviour of the hexacoordinate species is concerned, the TGA curve of [Ni(L)Py_3] above 100 °C (when the crystallisation pyridine molecules and both the axial pyridine molecules are lost) is the same as that of the square-planar complex [Ni(L)Py], as shown in Figure 3. From 220 to 250 °C a weight loss of about 11% is observed due to removal of coordinated pyridine from the square-planar complex and formation of a species that is stable up to 330 °C, which does not melt before decomposition. The elemental analysis of that species (a red crystalline product) is compatible with formation of the dinuclear [$Ni_2(L)_2$] species. Its TGA curve is shown in Figure 4. This behaviour suggests a good way to obtain [$Ni_2(L)_2$] species, since the methods described previously for other M^{II} ions[3c, 4a-4c] do not give products with a satisfactory degree of purity. Thermal treatment of [Ni(L)Py] at 270 °C for 3 min gave the dinuclear species quantitatively, which was then used in the grafting reaction onto the poly(4-vinylpyridine) (PVPy) backbones.

Grafted polymers were obtained by a bridge-splitting reaction of [$Ni_2(L)_2$] and anchoring of the Ni(L) fragments directly onto the pyridine nitrogens of the PVPy chains, as described previously.[4a–4c] Since a suitable choice of the molecular weight of the polymer backbone and of the grafting percentage of chromophoric fragment allows us to tune the spectroscopic, rheological, and thermodynamic properties of the final materials, two different compositions in complex (35% and 60% by weight) and two different molecular weights of PVPy (60000 and 160000) were studied. The latter choice was made in order to gain more viscous systems that are useful in the spin-coating deposition of polymeric thin films.

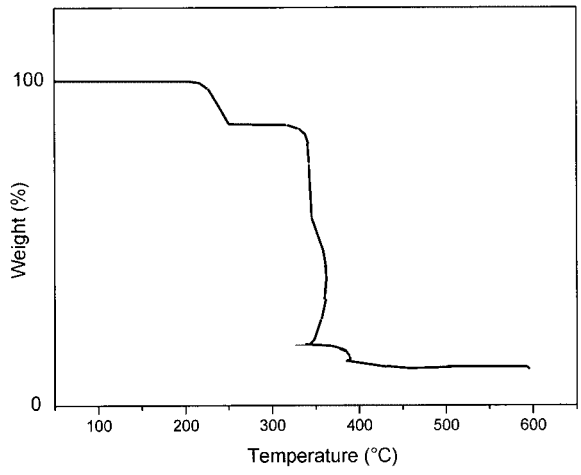

Figure 3. TGA curve of [Ni(L)Py] at a heating rate of 20 °C min^{-1}.

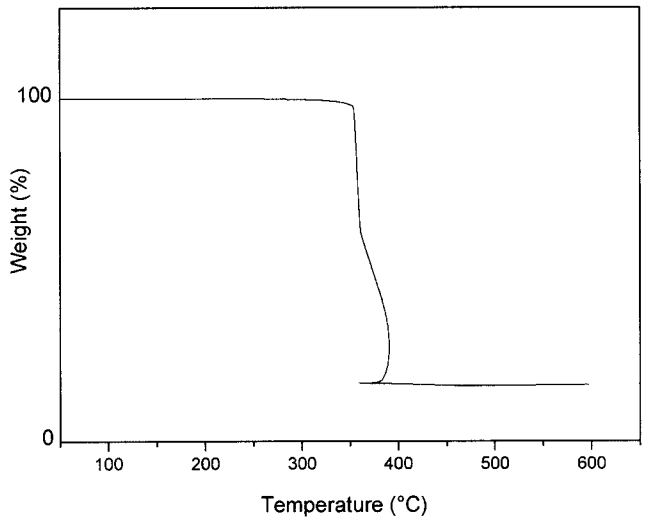

Figure 4. TGA curve of [$Ni_2(L)_2$] at a heating rate of 20 °C min^{-1}.

All the grafted PVPy samples are soluble in DMF and in *N*-methyl-2-pyrrolidinone. The ^{1}H NMR spectra of the four grafted PVPy samples, recorded in DMF solution, show broad peaks due to the high molecular weight of the polymers. No sharp peak pertaining to a free low-molecular-weight complex is detected. The signal at about δ = 8.5 ppm, due to the *ortho* hydrogen of the coordinated pyridine nitrogen, which occurs at about δ = 8.2 ppm in free PVPy and a peak at about δ = 3.4 ppm due to the –CH_2–*N*-φ protons in the chromophore, are the only significant resonances.

Table 2. Relevant spectroscopic and thermodynamic data for the polymers.

	T_g[a] [°C]	T_d[b] [°C]	η_{inh}[c] [dl/g]	%NiO_{calc}[d]	%NiO_{exp}[e]	ε[f] [L mol^{-1} cm^{-1}]	λ_{max}[g] [nm]	%NiL_{calc}[h]
PVPy60000	146[i]	360	0.27	–	–	–	–	–
[Ni(L)35PVPy60]	200	340	0.29	4.8	5.1	$4.0\cdot10^3$	360, 440	32
[Ni(L)60PVPy60]	243	332	0.37	7.6	8.6	$7.5\cdot10^3$	361, 440	59
PVPy160000	146[i]	360	0.51	–	–	–	–	–
[Ni(L)35PVPy160]	199	338	0.57	5.0	5.1	$4.6\cdot10^3$	360, 441	38
[Ni(L)60PVPy160]	244	335	0.60	7.2	8.6	$9.8\cdot10^3$	360, 442	58

[a] Glass-transition temperature. [b] Decomposition temperature (5% weight loss) in air. [c] Inherent viscosity (c = 50.0 mg mL^{-1}) in NMP at 60 °C. [d] Calculated metal content as NiO. [e] Experimental metal content as NiO. [f] Molar extinction coefficient. [g] Absorption maxima. [h] Coordinated fragment (as NiL) content calculated from absorbance values (on the basis of the absorbance of the dinuclear complex). [i] Dried at 200 °C.

The most relevant UV/Vis and thermodynamic data of the polymers are reported in Table 2. The values of the molar extinction coefficient from the UV/Vis spectra recorded in $CHCl_3$ solutions follow the chromophore content.

The glass-transition temperatures (T_g) increase with the grafting amount, and they are independent of the molecular weight of the polymer backbone. Remarkably, in this case we note a higher increase of the T_g with respect to analogous Cu^{II}- and Pd^{II}-grafted polymers.[4a–4c] In particular, the T_g values for both [Ni(L)35PVPy60] and [Ni(L)35PVPy160] are 53 °C above the value for free PVPy and those of [Ni(L)60PVPy60] and [Ni(L)60PVPy160] 98 °C above this value. For the Cu^{II}- and Pd^{II}-grafted PVPy (same ligand L), increases of 48 °C for both the 35% grafted polymers and only 74 °C for both the 60% ones were observed.[7]

UV/Vis absorption spectra for the mononuclear and the dinuclear species, the ligand and a metallated polymer (the curve for [Ni(L)35PVPy60] is reported as an example) are shown in Figure 5. As expected, the UV/Vis absorption pattern and λ_{max} value for the free ligand L are very different from those pertaining to the species containing L as a tridentate ligand, i.e. the mononuclear square-planar complex, the dinuclear complex and the grafted polymers, which are essentially identical. These spectra are also very similar to those we have recorded for complexes containing the same ligand and Cu^{II} or Pd^{II} metal ions.[4a] The UV/Vis spectra of the octahedral species are complicated by the various equilibria between adducts with different coordination geometry occurring in solution and also depend on the donor capability of the solvent.

The DSC curves for the two commercial PVPy samples and the corresponding grafted polymers are given in Figure 6. It should be noted that the signal due to the glass transition for a sample dried at 200 °C is very sharp (about 30 °C) in all cases. The larger increase in the T_g as compared with Cu^{II} and Pd^{II} systems[4a–4c] may be correlated with the tendency of the Ni^{II} ion to add two other pyridine molecules, thus promoting a stronger interaction between the polymer chains. Other experimental evidence of this behaviour is the observation that the solutions in which the grafting reaction was performed, and also the 10% solutions obtained by dissolving the metallated polymers at 200 °C to prepare spin-coated thin film samples, yield a gel upon quick cooling to room temperature.

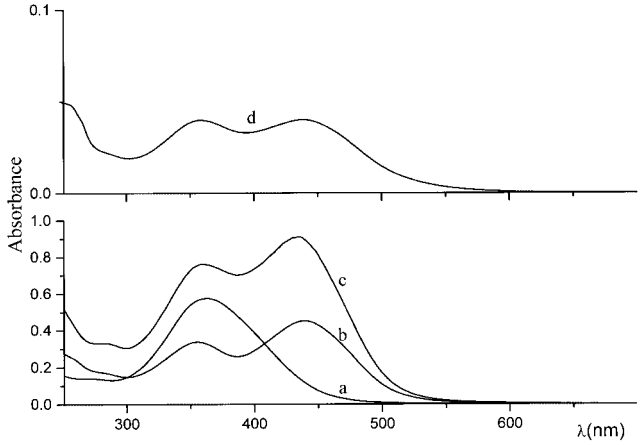

Figure 5. UV/Vis absorption spectra of L (curve a), [Ni(L)Py] (curve b), [$Ni_2(L)_2$] (curve c) and [Ni(L)35PVPy60] (curve d).

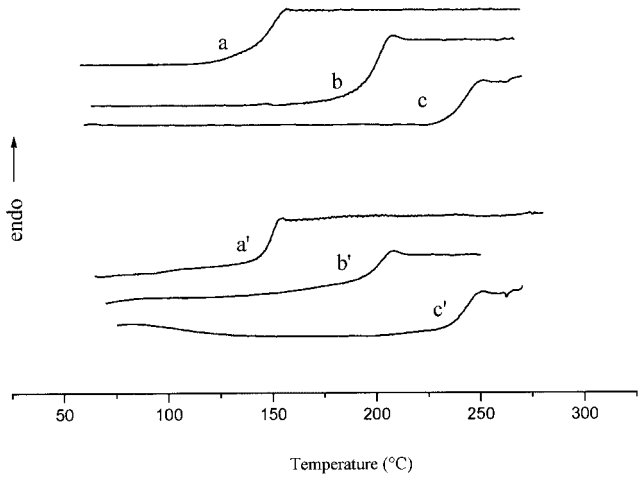

Figure 6. DSC curves (10 °C min^{-1}, N_2 atmosphere) for PVPy 60000 (a), [Ni(L)35PVPy60] (b), and [Ni(L)60PVPy60] (c), and PVPy 160000 (a′), [Ni(L)35PVPy160] (b′) and [Ni(L)60PVPy160] (c′).

Another point that is probably also related to the pyridine–metal interactions is the increase of the inherent viscosities with the grafting percentage with respect to that of free **PVPy**. In contrast, the inherent viscosities of the Cu^{II}-

and Pd^{II}-grafted PVPy samples decrease with the metal content.[4a–4c]

Thermal treatments of polymer samples simulating poling conditions (i.e. annealing near or above the T_g for 30 min) do not produce appreciable changes in their thermal behaviour. No evidence of crystallinity was detected in the subsequent DSC heating runs or by optical observations under a polarizing microscope. On a sample deposited as a thin film on a glass slide by the spin-coating technique from hot NMP solution, a transparent homogeneous surface was observed. X-ray spectra recorded for the untreated polymer samples show only haloes typical of an amorphous phase.

The high T_g values, the good thermal stability (decomposition temperatures are generally over 330 °C) and the absence of structured phases make these metallated polymers promising as materials for second order NLO applications. Moreover, the ability to establish interactions between the polymer chains (by metal coordination) could be used to obtain a kind of cross-linking at temperatures lower than the T_g, thus providing a stabilisation of the polar order of the chromophore units that is higher than in the analogous Cu^{II}- and Pd^{II}-grafted PVPy samples.

Conclusions

The use of a fragment containing the nickel(II) ion bound to a tridentate ligand in the preparation of grafted poly(4-vinylpyridine) samples for nonlinear optics affords significant improvements in the properties of the final materials. The ability of Ni^{II} to enlarge its coordination sphere is evidenced by the isolation and structural determination of a tetracoordinate square-planar model complex and of the corresponding hexacoordinate octahedral complex (resulting from addition of two other pyridine molecules to the first complex). The crosslinking related to the coordination expansion is reflected in the higher glass-transition temperatures of this series of metallated polymers and in the increase of their inherent viscosities. This should enhance the poling time stability.

Experimental Section

Materials: All solvents, poly(4-vinylpyridine) (PVPy; M_n = 60000 and 160000 uma), 4-diethylamino-2-hydroxybenzaldehyde, 4-nitrocinnamic acid and nickel(II) perchlorate hexahydrate are commercially available (Aldrich) and were used without purification.

Physical Measurements: Phase-transition temperatures and enthalpies were measured using a differential thermal analyzer DSC Perkin–Elmer Pyris (scanning rate 10 °C min^{-1}, nitrogen flow). Optical observations were performed with a Zeiss Axioscop polarizing microscope equipped with an FP90 Mettler temperature heating stage. UV/Vis absorption spectra were recorded at room temperature with a Jasco V-560 Spectrophotometer in DMF. IR spectra were recorded with a JASCO FP-750 apparatus. Thermogravimetric analysis was performed in air with a TA Instruments SDT 2960 with simultaneous DSC-TGA recording. ^1H NMR spectra were recorded by Varian spectrometers operating at 200 MHz or at 300 MHz. X-ray diffraction patterns were recorded on a flat film camera (Ni-filtered Cu-K_α radiation). The inherent viscosities of polymers (NMP solutions at 60.0 °C) were measured with an Ubbelohde viscometer.

Synthesis: Synthetic pathways for the metallated polymers [Ni(L)-PVPy] and for the dinuclear complex $[Ni_2(L)_2]$ and mononuclear complex [Ni(L)Py] are reported in Scheme 3. The synthesis of the ligand L has already been described by us.[4a]

[Ni(L)Py]: A solution of nickel(II) perchlorate hexahydrate (2.5 g, 6.84 mmol) in 20 mL of water was added at about 100 °C to a solution of L (3.0 g, 6.54 mmol) in 100 mL of pyridine. The resulting solution was stirred at 100 °C for about 10 min, after which time a dark-red solid precipitated upon further addition of water (about 80 mL). This solid was recovered by filtration and washed three times with water, then dried at 110 °C. Yield: 3.46 g (89%). Decomposition occurs before melting. $C_{31}H_{29}N_5NiO_4$: calcd. C 62.59, H 5.04, N 11.78; found C 62.58, H 4.98, N 11.68. Recrystallisation from $CHCl_3$/heptane gave brick-red crystals of [Ni(L)Py]. Single crystals for X-ray diffraction analysis were obtained from THF solution. ^1H NMR (200 MHz, $CDCl_3$, Me_4Si): δ = 8.68 (d, 2 H), 8.20 (d, 2 H), 7.92 (d, 2 H), 7.76 (s, 1 H), 7.63 (d, 2 H), 7.48 (m, 4 H), 7.19 (m, 3 H), 6.22 (s, 1 H), 6.17 (s, 2 H), 3.346 (q, 4 H), 1.17 (t, 6 H) ppm.

[Ni(L)Py_3]: Dark-violet crystals of the hexacoordinate complex were obtained by slow evaporation of a pyridine solution of [Ni(L)Py]. The sample was stored at room temperature under pyridine atmosphere for further characterisations.

[$Ni_2(L)_2$]: This dinuclear complex was obtained by thermal treatment of the mononuclear complex [Ni(L)Py] at 270 °C for 3 min. The resulting dark-red crystals were used without further treatment. Yield: quantitative. Decomposition occurs before melting. $C_{52}H_{48}N_8Ni_2O_8$: calcd. C 60.56, H 4.85, N 10.87; found C 60.44, H 4.80, N 10.79.

Ni(L)PVPy: Four polymers {[Ni(L)35PVPy60], [Ni(L)60PVPy60], [Ni(L)35PVPy160] and [Ni(L)60PVPy160]} were obtained by grafting the fragment Ni(L) (at 35% and 60% by weight) onto two PVPy samples (60000 and 160000 average molecular weight). The polymers were prepared following a synthetic procedure already described by the authors,[4b] by dissolving the appropriate amount of PVPy (previously dried at 200 °C) in DMF and the dimeric complex $[Ni_2(L)_2]$ in DMF and blending and stirring the solution for 25 min at 90 °C. The polymer that precipitated upon addition of water was washed twice with vigorous stirring and dried at 120 °C. The yield was quantitative.

[Ni(L)35PVPy160]: Calcd. C 72.37, H 6.02, N 12.46; found C 71.00, H 6.16, N 12.22.

[Ni(L)35PVPy60]: Calcd. C 72.37, H 6.02, N 12.46; found C 70.38, H 6.12, N 12.08.

[Ni(L)60PVPy60]: Calcd. C 68.26, H 5.57, N 11.84; found C 67.80, H 5.60, N 11.85.

[Ni(L)60PVPy160]: Calcd. C 68.26, H 5.57, N 11.84; found C 67.65, H 5.68, N 11.76.

X-ray Analysis: X-ray data collection for [Ni(L)Py] was performed at room temperature on an Enraf–Nonius MACH3 diffractometer in the ω/θ scan mode, using graphite-monochromated Mo-K_α radiation (λ = 0.71069 Å). Cell parameters were obtained from a least-squares fit of the θ angles of 25 reflections in the range 7.04° $\leq \theta \leq$ 8.95°. A semi-empirical absorption correction (ψ scans) was applied.

Data collection for $Ni(L)Py_3$ was performed at low temperature (–100 °C) on a Bruker–Nonius kappa CCD diffractometer (Mo-K_α

radiation, phi scans + omega scans to fill the asymmetric unit). Cell parameters were obtained from a least-squares fit of the θ angles of 30 reflections in the range $6.02° \leq \theta \leq 9.89°$. A semi-empirical absorption correction (multiscan, SADABS) was applied.

Both structures were solved by direct methods and refined anisotropically by the full-matrix least-squares method on F^2 against all independent measured reflections (SHELXS and SHELXL program of the SHELX 97 package[8]). H atoms were placed in calculated positions as riding on their carriers atoms. Max. residual electron density 0.691 (–0.424) e Å^{-3} for [Ni(L)Py] and 0.315 (–0.333) e Å^{-3} for [Ni(L)Py$_3$]. Some crystal, collection and refinement data are reported in Table 3.

Table 3. Crystallographic data collection and refinement for [Ni(L)Py] and [Ni(L)Py$_3$].

	[Ni(L)Py]	[Ni(L)Py$_3$]
Chemical formula	$C_{31}H_{29}N_5NiO_4{\cdot}C_4H_8O$	$C_{41}H_{39}N_7NiO_4{\cdot}2.5(C_5H_5N)$
Formula mass	666.41	950.25
T [K]	293	173
Crystal system	triclinic	orthorhombic
Space group	$P\bar{1}$	$Fdd2$
a [Å]	9.667(9)	42.992(5)
b [Å]	11.61(1)	50.457(5)
c [Å]	15.83(1)	9.101(3)
α [°]	71.93(6)	90
β [°]	86.04(5)	90
γ [°]	72.70(7)	90
V [Å^3]	1606(2)	19710(7)
Z, $D_{calcd.}$ [g cm^{-3}]	2, 1.373	16, 1.281
μ [mm^{-1}]	0.655	0.449
Theta range	1.36°, 27.93°	3.05°, 25.02°
Data/parameters	7709/415	7671/614
R_1 [$I > 3\sigma(I)$]	0.0631	0.0462
R_1, wR_2 (all data)	0.1904, 0.2346	0.2227, 0.1124

$$R1 = \frac{\sum \left| |F_o| - |F_c| \right|}{\sum |F_o|} \quad ; \quad wR2 = \left\{ \frac{\sum \left[w\left(F_o^2 - F_c^2\right)^2 \right]}{\sum \left[w\left(F_o^2\right)^2 \right]} \right\}^{1/2}$$

CCDC-249658 (for [Ni(L)Py]) and CCDC-249659 (for [Ni(L)Py$_3$]) contain the supplementary crystallographic data for this paper. These data can be obtained free of charge from The Cambridge Crystallographic Data Centre via www.ccdc.cam.ac.uk/data_request/cif.

NLO Characterisation: The second-order optical nonlinearity of [Ni(L)Py] was determined by the EFISH technique, in chloroform, by measuring the $\mu_g\beta$ dot product of the chromophore, where μ_g is the ground state permanent dipole moment and β the (vector) quadratic hyperpolarizabilty of the molecule. The light source was a Q-switched Nd:Yag laser whose emission at 1.06 μm was shifted to 1.907 μm by stimulated Raman scattering in a high-pressure hydrogen cell. The measurements were calibrated relative to a quartz wedge: the experimental value of $d_{11}^{quartz} = 1.2 \times 10^{-9}$ esu at 1.06 μm was extrapolated to 1.1×10^{-9} esu at 1.907 μm. A detailed description of the experimental apparatus is given elsewhere.[9]

Acknowledgments

We thank the CIMCF of the Università di Napoli "Federico II" for X-ray (MACH 3) and NMR facilities and the C.R.d.C. "Nuove Tecnologie per le attività produttive" (Regione Campania, Italy) for the Nonius kappa-CCD diffractometer. Financial support from MIUR (Italy) within FIRB2001 grant is also acknowledged. Thanks are due to Dr. Alain Fort of IPCMS-CNRS GONLO of Strasbourg (France) for help with the EFISH measurements.

[1] a) T. D. Trouts, D. S. Tyson, R. Pohl, D. V. Kozlov, A. G. Waldron, F. N. Castellano, *Adv. Funct. Mater.* **2003**, *13*, 398; b) W.-J. Kuo, G.-H. Hsiue, R.-J. Jeng, *Macromolecules* **2001**, *34*, 2373; c) R. J. Forster, J. G. Vos, *Macromolecules* **1990**, *23*, 4372.

[2] a) S. Di Bella, I. Fragalà, *Synth. Met.* **2000**, *115*, 191; b) X. T. Tao, H. Suzuki, T. Watanabe, S. H. Lee, S. Miyata, H. Sasabe, *Appl. Phys. Lett.* **1997**, *70*, 1503.

[3] a) F. Cariati, U. Caruso, R. Centore, A. De Maria, M. Fusco, B. Panunzi, A. Roviello, A. Tuzi, *Inorg. Chim. Acta* **2004**, *357*, 548; b) I. Aiello, U. Caruso, M. Ghedini, B. Panunzi, A. Quatela, A. Roviello, F. Sarcinelli, *Polymer* **2003**, *44*, 7635; c) Special publication: W. Chiang, M. E. Thompson, D. Van Engen, *Spec. Publ. – R. Soc. Chem.* **1991**, *91* (Org. Mater. Non-linear Opt. 2), 210.

[4] a) F. Cariati, U. Caruso, R. Centore, W. Marcolli, A. De Maria, B. Panunzi, A. Roviello, A. Tuzi, *Inorg. Chem.* **2002**, *41*, 6597; b) U. Caruso, A. De Maria, B. Panunzi, A. Roviello, *J. Polym. Sci., Polym. Chem. Ed.* **2002**, *40*, 2987; c) F. Borbone, U. Caruso, R. Centore, A. De Maria, A. Fort, M. Fusco, B. Panunzi, A. Roviello, A. Tuzi, *Eur. J. Inorg. Chem.* **2004**, 2467.

[5] a) M. Yang, L. Zhang, Z. Lei, P. Ye, J. Si, Q. Yang, Y. Wang, *J. App. Polym. Sci.* **1998**, *70*, 1165; b) M. J. Yang, K. Ding, L. J. Zhang, W. G. Chen, *Synth. Met.* **1995**, *71*, 1739; c) A. Borshch, M. Brodyn, V. Lyakhovetsky, V. Volkov, A. Kutsenko, S. Maloletov, *Mater. Sci.* **2002**, *20*, 29.

[6] a) A. E. Underhill, C. A. S. Hill, *Mol. Cryst. Liq. Cryst. Sect. A* **1992**, *217*, 7; b) C. S. Winter, S. N. Oliver, J. D. Rush, C. A. S. Hill, A. E. Underhill, *J. Appl. Phys.* **1992**, *71*, 512.

[7] A. Roviello and co-workers, unpublished results.

[8] G. M. Sheldrick, SHELX-97, University of Göttingen, Germany, **1997**.

[9] T. Thami, P. Bassoul, M. A. Petit, J. Simon, A. Fort, M. Barzoukas, A. Villaeys, *J. Am. Chem. Soc.* **1992**, *114*, 915.

Received: October 26, 2004
Published Online: June 3, 2005

